

## 유한 요소법을 이용한 비선형 슬러싱 문제 해석

경조현<sup>1†</sup> · 김장환<sup>2</sup> · 조석규<sup>1</sup> · 배광준<sup>3</sup>

<sup>1</sup>한국해양연구원, <sup>2</sup>미국선급협회, <sup>3</sup>서울대학교

# Numerical Analysis on Nonlinear Sloshing Problem using Finite Element Method

Jo-Hyun Kyoung<sup>1†</sup>, Jang-Whan Kim<sup>2</sup>, Seok-Kyu Cho<sup>1</sup> and Kwang-June Bai<sup>3</sup>

<sup>1</sup>Ocean Development System Research Division, Korea Research Institute of Ships & Ocean Engineering, KORDI, Jang-Dong, Yuseong-Gu, Daejeon 305-343, Korea

<sup>2</sup>American Bureau of Shipping, 16855 Northchare DR., Houston, TX, USA

<sup>3</sup>Department of Naval Architecture & Ocean engineering, Seoul National University, San 56-1, Sillim-Dong, Gwanak-Gu, Seoul 151-744, Korea

### 요 약

본 논문에서는 3차원 비선형 슬러싱 유동에 대한 수치해법을 개발하였다. 탱크내에서 과도한 슬러싱 유동이 일어나는 경우에는 슬러싱 유동에 의해 유기되는 유체 충격력에 의해 탱크 내부 부재나 탱크 자체의 손상을 야기할 수 있다. 비선형 슬러싱 유동을 포텐셜 유동 이론에 근거한 자유표면과 문제로 정식화하고, 엄밀한 비선형 자유표면 경계조건을 적용하여 수치적으로 해석하였다. 안정된 수치 해법 개발을 위해 해밀톤 원리에 근거한 변분법을 사용하였으며 얻어진 변분식에 유한 요소법을 적용하여 해석하였다. 비선형 자유표면 유동은 시간영역에서의 초기치 문제로 해석하였으며 자유표면의 위치는 매 계산 시간 간격마다 반복계산에 의해 결정되었다. 수치 해석 결과로는 탱크 내에 위치한 파이프에 비선형 슬러싱 유동에 의해 야기되는 유체 충격력을 구하였다.

**Abstract** – A nonlinear sloshing problem is numerically simulated. During excessive sloshing the sloshing-induced impact load can cause a critical damage on the tank structure. A three-dimensional free-surface flow in a tank is formulated in the scope of potential flow theory. The exact nonlinear free-surface condition is satisfied numerically. A finite-element method based on Hamilton's principle is employed as a numerical scheme. The problem is treated as an initial-value problem. The computations are made through an iterative method at each time step. The hydrodynamic loading on the pillar in the tank is computed.

**Keywords:** Nonlinear sloshing problem(비선형 슬러싱 문제), Nonlinear Free-surface flow(비선형 자유표면과 문제), Finite element method(유한요소법), Wave impact(파랑 충격력)

### 1. Introduction

Sloshing is a phenomenon of great engineering importance in the fields of naval architecture, ocean engineering and civil engineering. A severe sloshing can occur in a large oil storage tank, a reservoir and a fuel tank. An excessive sloshing motion in LNG tanker can rupture the pipeline in a tank and tank itself. The results of several research programs investigating sloshing in Liquefied Natural Gas (LNG) Carriers are presented in Abram-

son *et al.* (1974). In the study, the history of slosh-related problems in LNG carriers is discussed including a list of recorded tank damages for LNG sloshing when the filling height is low and high relative to the tank length. In both cases impact loads and the induced extremely high pressures have been reported.

There have been a considerable number of investigations on a sloshing problem. For the case of small amplitude excited motions, Solaas & Faltinsen (1997) adopted a perturbation theory. For large amplitude excited motions, Jones & Hulme (1987), Faltinsen (1974, 1978), Okamoto & Kawahara (1990),

<sup>†</sup>Corresponding author: johyun@kriso.re.kr

Chen *et al.* (1996), Armenio & La Rocca (1996) used various numerical methods for a two dimensional problem, Huang & Hsiung (1996) used a shallow water equation. Wu *et al.* (1996) simulated sloshing in a 3D tank using finite element method for a potential flow model. Ferrant & Le Touze (2001) applied an inviscid pseudo-spectral model to predict 3D sloshing. Ushijima (1998) used an Arbitrary Lagrangian-Eulerian method on boundary-fitted grids to analyse viscous and swirling effects in a 3D cylindrical tank. Wu *et al.* (2001) derived an analytical solution for a sloshing problem in a rectangular tank including viscosity.

Especially at a low filling rate (approximately 5-20%) from experimental observations of Verhagen & Wijngaarden (1965), Vander Bosch & Vugts (1966), Chester (1968), Chester & Bones (1968), and Adee & Caglayan (1982), the wave elevation in a tank has the same magnitude as that of the water depth in vicinity of resonant frequencies. In addition to that, a very steep wave front like a hydraulic jump has been observed in experiments. The bore traveled back and forth between the tank walls. This introduces difficulties in establishing a stable numerical scheme and in capturing highly nonlinear free surface phenomena, i.e., the discontinuous hydraulic jump. When the waves are overturning and hitting the water surface, air bubbles may be present in the fluid. In this case, a direct numerical solution based on potential flow made with the nonlinear free surface conditions would break down. Another difficulties such as hydroelasticity will also occur when the water impact against the wall and the top of the tank.

In order to overcome these difficulties, we employed a finite element formulation based on Hamiltons variational principle, which provides a stable numerical solution. This approach has been already applied to the nonlinear free surface problems successfully (Bai *et al.*, 1989, 1994, 1995, 2002). A preliminary result of the present numerical method was reported in Bai *et al.* (2002). In the present study, we introduced the diffusive damp-

ing term to make the steep bore smooth. Our numerical model is an open-type tank without a roof. Main focus is made on the prediction of the impact force on the pillar located in the middle of the tank by the bore induced by a large amplitude sway motion.

## 2. MATHEMATICAL FORMULATION

The Cartesian coordinate system is adopted.  $Oxyz$  is the coordinate system fixed on the tank with  $Oz$  opposing the direction of gravity and  $z=0$  coincides the undisturbed free surface. The tank is subjected to a sway motion with amplitude  $A$  and frequency  $\omega$ .

It is assumed that the fluid is inviscid, incompressible and its motion is irrotational. So the velocity potential can be defined as

$$u(\vec{x}, t) = \nabla\phi(\vec{x}, t) \tag{1}$$

where  $\vec{x} = (x, y, z)$  and  $\phi$  is the velocity potential. From the continuity condition we obtain the Laplace equation

$$\nabla^2\phi(\vec{x}, t) = 0 \text{ in fluid domain } D \tag{2}$$

The boundary condition on the body boundary ( $S_B$ ) is

$$\phi_n = 0 \quad \text{on} \quad S_B \tag{3}$$

where the vector,  $\vec{n} = (n_x, n_y, n_z)$ , denotes the outward unit normal vector on the boundaries. The conditions on the free surface, i.e.  $z=\zeta(x, y, t)$ , can be given by the kinematic and dynamic boundary conditions as follows.

$$\zeta_t = \frac{1}{n_z} \phi_n \tag{4}$$

$$\phi_t = -\frac{1}{2}|\nabla\phi|^2 - g\zeta - \frac{p}{\rho} - x\frac{du}{dt} \tag{5}$$

$$n_z = 1/\sqrt{1 + \zeta_x^2 + \zeta_y^2} \tag{6}$$

Here  $g$  and  $\rho$  denote the gravitational acceleration and the density of fluid, respectively. The pressure  $p=p(x, y, t)$  is taken zero unless a non-zero pressure distribution is specified. The displacement of the tank is given as  $x_B=A \cos \omega t$ . Then the velocity of the tank is  $u=dx_B/dt = -A\omega \sin \omega t$ . The resonant frequency  $\omega$  is obtained from the dispersion relation, i.e.,  $w^2=gk \tanh kh$ . It is interesting that the last term in Equation (5) behaves like a pressure. The fluid motion is assumed to be at rest initially. Therefore the initial condition may be given as

$$\phi = \phi_t = 0 \quad \text{at} \quad t=0 \tag{7}$$

The depth of water is  $h$  and the tank width is  $B$ . The wall

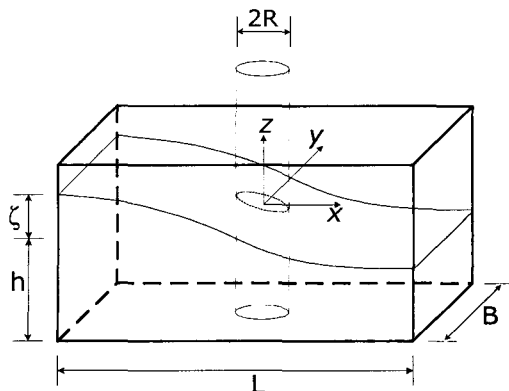


Fig. 1. Coordinate system.

boundary conditions are given as follows.

$$\phi_n = 0 \quad \text{on} \quad z = -h \quad (8)$$

$$\phi_n = 0 \quad \text{on} \quad y = \pm B/2 \quad \text{and} \quad x = \pm L/2 \quad (9)$$

### 3. VARIATIONAL FORMULATION

We introduce a variational formulation which is equivalent to the above problem without sway motion. The last term in Eq. (5) induced by sway motion can be replaced by pressure term. Let the gravitational acceleration term,  $g$ , be unity. First we define the variational functional,  $J$  and the Lagrangian  $L$  as

$$J = \int_0^{t^*} L dt \quad (10)$$

$$L = \iint_{\bar{S}_F} \phi \zeta_s dS - \frac{1}{2} \iint_{\bar{S}_F} g \zeta^2 dS - \frac{1}{2} \iiint_D |\nabla \phi|^2 dV \quad (11)$$

where  $\bar{S}_F$  is the projection of  $S_F$  on Oxy plane and  $t^*$  is the final time. Taking the variations on  $J$  first with respect to  $\zeta$ , we can obtain  $\delta J_\zeta$  as

$$\begin{aligned} \delta J_\zeta &= \int_0^{t^*} dt \left[ \iint_{\bar{S}_F} \left( \phi \delta \zeta_s - g \zeta \delta \zeta - \frac{1}{2} |\nabla \phi|^2 \delta \zeta \right) dS \right] \\ &= \iint_{\bar{S}_F} [\phi \delta \zeta]_{t=0}^{t^*} - [\phi \delta \zeta]_{t=0} dS - \int_0^{t^*} dt \left[ \iint_{\bar{S}_F} \left( \phi_s + \frac{1}{2} |\nabla \phi|^2 + g \zeta \right) \delta \zeta dS \right] \end{aligned} \quad (12)$$

Next the variations on  $J$  with respect to  $\phi$ , i.e.,  $\delta J_\phi$  can be obtained as

$$\begin{aligned} \delta J_\phi &= \int_0^{t^*} dt \left[ \iint_{\bar{S}_F} \zeta_s \delta \phi dS - \iiint_D \nabla \phi \cdot \nabla \delta \phi dV \right] \\ &= \int_0^{t^*} dt \left[ \iint_{\bar{S}_F} \left( \zeta_s - \frac{1}{n_z} \phi_n \right) \delta \phi dS + \iiint_D \nabla^2 \phi \delta \phi dV \right] \end{aligned} \quad (13)$$

Here  $\delta J = \delta J_\zeta + \delta J_\phi$ . Eq. (12) means that the stationary condition on  $J$  for the variation with respect to  $\zeta$  recovers the dynamic free surface condition in each time and that the wave elevation at  $t=0$ ,  $t^*$  should be specified as the constraints. Eq. (13) shows that the stationary condition on  $J$  for the variation of  $\phi$  recovers the kinematic condition on  $S_F$  and the governing equation. The above variational form is previously given by Miles (1977) and is slightly different from that given by Luke (1967). In the present variational formulation the wave elevation  $\zeta$  assumed to be known at  $t=0$ ,  $t^*$  whereas Luke assumed the potential  $\phi$  to be known at both initial and final times additionally. The present functional has an advantage over the original Luke's variational functional in treating the nonlinear free surface boundary conditions.

### 4. FINITE-ELEMENT DISCRETIZATION

In the original initial/boundary-value problem, the admissible function should be twice continuously differentiable. But in the above variational method, it is sufficient that the admissible trial functions have the square integrable properties of the function  $\phi$  and its first derivatives in space. This fact enables us to seek an approximate solution in a wider class in the variational method. As the first step in the numerical procedure, the fluid domain is to discretize into finite number of finite elements. In this study, the finite elements are generated such that projections of  $x$  and  $y$  coordinates on the horizontal plane are fixed but the other coordinate, i.e. the  $z$ -axis, is allowed to move vertically in time. This restriction makes the regridding and computation considerably simple. But, it is not always necessary to impose this restriction in general. The trial basis is denoted by  $\{N_i\}_{i=1,\dots,N}$  and  $\zeta$  is approximated by the span of the bases,  $\{N_i\}_{i=1,\dots,N}$  on  $S_F$  which is also continuous and piecewise differentiable on  $\bar{S}_F$ . Then the potential function and the wave elevation can be represented as

$$\phi(x, y, z, t) = \phi_s(t) N_i(x, y, z; \zeta) \quad (14)$$

$$\zeta(x, y, t) = \zeta_s(t) M_k(x, y) \quad (15)$$

where

$$M_k(x, y) = N_i(x, y, z; \zeta)|_{z=\zeta}, k = 1, \dots, N_F \quad (16)$$

Einstein's summation convention for the repeated indices is used here.  $N_F$  is the number of nodal point on  $S_F$  and  $i_k$  is the nodal number of the basis function  $N_i$  of which the node coincides with that of the free surface node  $k$ . It should be noted that the basis function,  $\{N_i\}_{i=1,\dots,N}$ , is dependent on the free surface shape,  $z = \zeta$ , but its restriction on  $S_F$  is the function of  $(x, y)$  and independent of  $\zeta$ . The special property of  $\{M_k\}_{k=1,\dots,N_F}$  is resulted from the finite-element subdivision employed here. Once the trial function is approximated by using the above basis function, the Lagrangian,  $L$ , for these trial solutions are obtained as

$$L = \phi_i T_{ij} \zeta_j - \frac{1}{2} \phi_i K_{ij} \phi_j - \frac{1}{2} g \zeta_k P_{kj} \zeta_j \quad (17)$$

$$T_{ij} = \iint_{\bar{S}_F} M_k M_j dS \quad (18a)$$

$$P_{kj} = \iint_{\bar{S}_F} M_k M_j dS \quad (18b)$$

$$K_{ij} = \iiint_D \nabla N_i \cdot \nabla N_j dV \quad (18c)$$

The tensors,  $K_{kj}$ ,  $P_{kj}$  are the kinetic and potential energy tensor and  $T_{kj}$  is a tensors obtained from the free surface integral,

which can be interpreted as a tensor related to the transfer rate between these two energies. It is of interest to note that in Eq. (18),  $T_{kj}=P_{kj}$ . The stationary condition on  $J=\int Ldt$  gives the following Euler-Lagrange equation.

$$T_{kj}\zeta_j = K_{ij}\phi_j \quad (19)$$

$$T_{kj}\dot{\phi}_i = -\frac{1}{2}\phi_i\frac{\partial K_{ij}}{\partial \zeta_k}\phi_j - gP_{kj}\zeta_j \quad \text{for } k=1, \dots, N_F \quad (20)$$

$$K_{ij}\phi_j = 0, \quad i \neq i_k \quad (21)$$

Here Eq. (19) and Eq. (20) are the nonlinear ordinary differential equation for  $\{\zeta_k, \phi_i\}_{k=1, \dots, N_F}$  and Eq. (21) is the algebraic equations for  $\{\phi_i\}_{i \neq i_k}$  which is the constraints for the above two equations. It can be easily shown that the solution of the above discretized problem satisfies the conservation of mass and total energy, i.e.

$$\frac{d}{dt}\left(\sum_{k,j} P_{kj}\zeta_j\right) = 0 \quad (22)$$

$$\frac{d}{dt}\left(\sum_{i,j} \phi_i K_{ij}\phi_j + \sum_{k,j} \zeta_j P_{kj}\zeta_j\right) = 0 \quad (23)$$

This property of the conservations is independent of the tensor  $T_{ij}$  if it satisfies

$$\sum_k T_{kj} = \sum_k P_{kj} \quad (24)$$

It should be also pointed out that the direct use of Eq. (20) leads to some difficulty in the computations. This difficulty arises from the first term in the right-hand side which is the derivative of the kinetic energy tensor with respect to the wave elevation. We have avoided this difficulty by utilizing the fact that Eq. (20) is equivalent to the condition of vanishing of the right-hand side in Eq. (12). In Eq. (12),  $\delta\zeta$  can be regarded as test functions on  $\bar{S}_F$ . Then Eq. (20) can be given as

$$T_{jk}\dot{\phi}_i = -\iint_{\bar{S}_s} M_j\phi_i\zeta_j dS - \frac{1}{2}\iint_{\bar{S}_s} M_j|\nabla\phi|^2 dS - gP_{jk}\zeta_k \quad (25)$$

$\delta\phi$  can also be regarded as test functions on  $\bar{S}_F$  in Eq. (13). Therefore Eq. (21) can be given as

$$T_{jk}\zeta_i = \iint_{\bar{S}_s} M_j\phi_i/n_z dS \quad (26)$$

Consequently, the Laplace equation in Eq. (21) is no more than a constraint. In order to make the first derivative terms of  $\phi$  written as terms on the free surface, we utilized the same relations as Zakharov (1968). Then our system becomes Hamiltonian.

$$\phi_i(x, y, z, t) = \phi_i(x, y, \zeta(x, y, t), t) + \phi_i\zeta_i \quad (27)$$

$$\phi_i(x, y, z, t) = \phi_i(x, y, \zeta(x, y, t), t) + \phi_i\zeta_i \quad (28)$$

$$\phi_i(x, y, z, t) = \phi_i(x, y, \zeta(x, y, t), t) + \phi_i\zeta_i \quad (29)$$

Using above relation, we can rewrite Eq. (25) as

$$T_{jk}\dot{\phi}_i = \frac{1}{2}\iint_{\bar{S}_s} M_j\left[n_z^2\left(\frac{\phi_n}{n_z} + \nabla_s\phi \cdot \nabla_s\zeta\right)^2 - \nabla_s\phi \cdot \nabla_s\phi\right] dS - gP_{jk}\zeta_k \quad (30)$$

where  $\nabla_s = \left(\frac{\partial}{\partial x}, \frac{\partial}{\partial y}\right)$  and  $n_z = 1/\sqrt{1 + \zeta_x^2 + \zeta_y^2}$ .

If the integrals in Eq. (20) and Eq. (30) and the integrals in Eq. (19) and Eq. (26) are evaluated exactly, they are equivalent. However, in the present computation these integrals are calculated by integral quadrature rules. Therefore, the conservation of energy may not be satisfied exactly due to the error caused by the numerical integration.

## 5. NUMERICAL INSTABILITY

The potential theory does not have any mechanism for energy dissipation inside a tank. This means that a steady-state solution may be difficult to obtain when a forced harmonic oscillation of the tank is imposed in the vicinity of the natural modes. In model tests by Faltinsen (1974), the fluid motion was observed to oscillate finally with the same period as the forced oscillation. This implies that the damping is present in reality. To simulate the effect of viscous damping in the potential theory model, an artificial damping term may be introduced. For this reason, Faltinsen (1978) introduced the artificial damping term on the dynamic free surface condition.

$$\phi_i = -\frac{1}{2}|\nabla\phi|^2 - g\zeta - \frac{\rho}{\rho} - \mu\phi \quad (33)$$

This term helps the wave motion become steady oscillatory. However, that artificial damping can not represent the real physical viscous damping. In addition to that, it has a tendency to make whole system damped out.

As an alternative damping mechanism to prevent from breaking, we introduced the diffusive damping terms in the free surface conditions as follows.

$$\zeta_i = \frac{1}{n_z}\phi_n + \mu\nabla_s^2\zeta \quad (34)$$

$$\phi_i = -\frac{1}{2}|\nabla\phi|^2 - g\zeta - \frac{\rho}{\rho} - \mu\nabla_s^2\phi \quad (35)$$

The last terms in the right-hand side in Eq. (34) and Eq. (35) are the diffusive terms. An introduction of these terms also plays a role of an artificial diffusion on the free surface. When the other numerical schemes experience the steep wave like a bore, these terms will prevent the wave from steepening. A brief

background of adopting these diffusive terms is given in Appendix. The damping coefficient  $\mu$  depends on the size of grid, integration time interval and steepness of bore. It is difficult to take accurate value of the damping coefficient. Therefore the appropriate damping coefficient is taken by trial and error.

## 6. TIME INTEGRATION ON THE FREE SURFACE

Once we discretize the computational domain into a number of finite elements and perform integrations in term of three space variables, we obtain a set of ordinary differential equations in matrix form given as follows.

$$T_{kj}\dot{\zeta}_j = -\mu C_{kj}^s \zeta_j + T_{kj} \frac{\dot{\phi}_i}{n_{z,j}} \quad (36)$$

$$T_{kj}\dot{\phi}_i = -\mu C_{kj}^o \phi_j + \frac{1}{2} \tilde{C}_{kij}(\phi_i, \zeta_j) - g P_{kj} \zeta_j \quad (37)$$

$$K_{ij}\phi_j = 0 \quad (38)$$

The coefficients are defined as

$$C_{kj}^s = \iint_{\bar{S}_s} \nabla_s N_k \cdot \nabla_s N_j dS \quad (39)$$

$$C_{kj}^o = \iint_{\bar{S}_s} \nabla_s N_k \cdot \nabla_s N_j dS \quad (40)$$

$$\tilde{C}_{kij}(\phi_i, \zeta_j) = \iint_{\bar{S}_s} M_k \left[ n_z^2 \left( \frac{\dot{\phi}_i}{n_z} + \nabla_s \phi \cdot \nabla_s \zeta \right) - \nabla_s \phi \cdot \nabla_s \phi \right] dS \quad (41)$$

It should be pointed out that Eq. (38) can be interpreted as a constraint to Eq. (36) and Eq. (37). Eq. (38) is obtained from the boundary value problem with an essential condition (Dirichlet type) on free surface and a natural condition (Neumann type) on the body surface.

In the solution procedure, the constraint, i.e., Eq. (38) is first

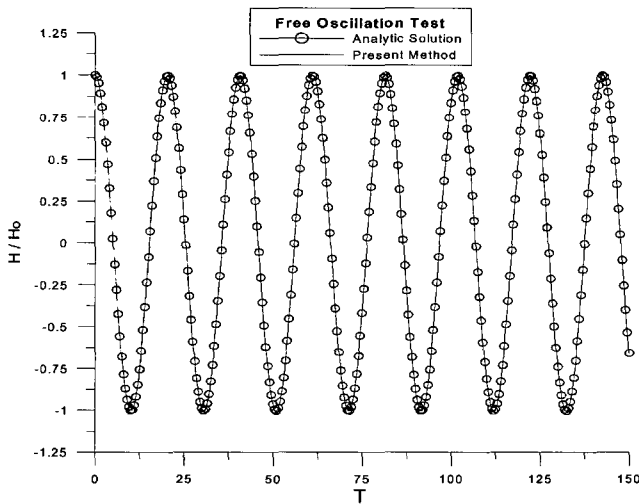


Fig. 2. Free oscillation test.

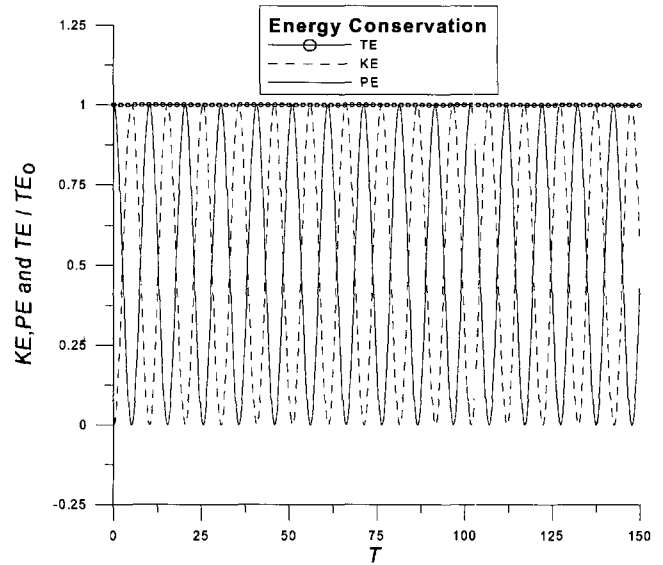


Fig. 3. Energy conservation.

solved by the GMRES (Generalized Minimal RESidual, Saad & Schultz, 1986) algorithm. Then the matrix  $T_{kj}$  is inverted by the same method. Here the other matrices, which are dependent on the free surface shape, are treated as known values from the previous time step. The final form in Eq. (36) and Eq. (37) is solved by the fourth-order Runge Kutta method.

## 7. RESULTS AND DISCUSSION

Before we made computations for the sloshing problem in the tank, a series of tests was conducted for two-dimensional free oscillations. The computed result for the conservation of energy in the case of two-dimensional free oscillations is given in Fig. 2 and Fig. 3.

In the computations the length of tank is taken to be 10 m with the water depth  $h$  being 1 m. Initial wave height is taken as  $1/1000 h$ . Time integration step is  $1/50$  second. The number of elements in horizontal and the vertical directions are 40, 15, respectively. This scheme conserves energy with a good accuracy and agrees well with the analytic solution.

For the sloshing problem in a tank with a pillar in the middle of the tank, the computations are made for the conditions given

Table 1. Computational Cases for sloshing tank with a pillar

$L$	$B$	$h$	$R$	$A$	$\mu$	$\Delta t$
40 m	10 m	1 m	1.5 m	1.5 m	1.0	0.0511
40 m	10 m	2 m	1.5 m	1.5 m	1.5	0.0363
40 m	10 m	3 m	1.5 m	1.5 m	2	0.0149
40 m	10 m	4 m	1.5 m	1.5 m	2	0.0130

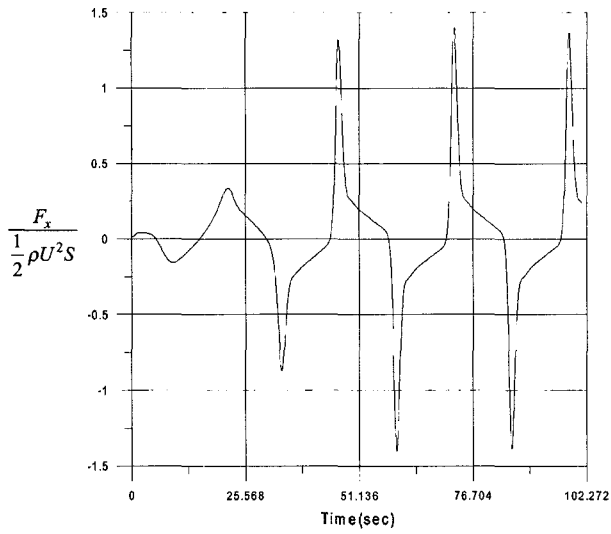


Fig. 4. Impact force on the pillar versus time:  $h=1$  m.

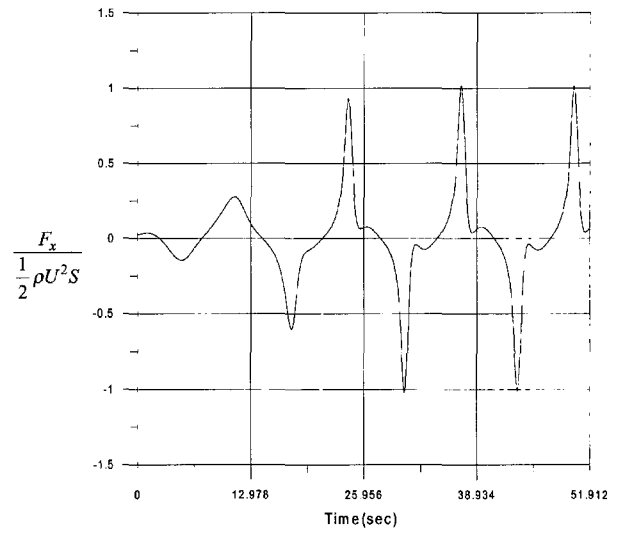


Fig. 7. Impact force on the pillar versus time:  $h=4$  m.

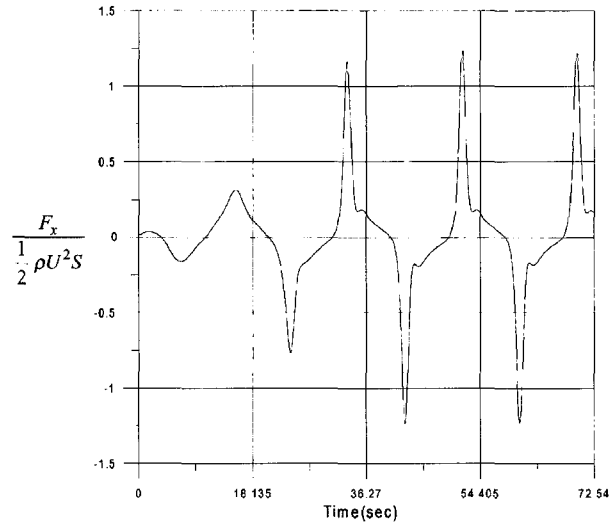


Fig. 5. Impact force on the pillar versus time:  $h=2$  m.

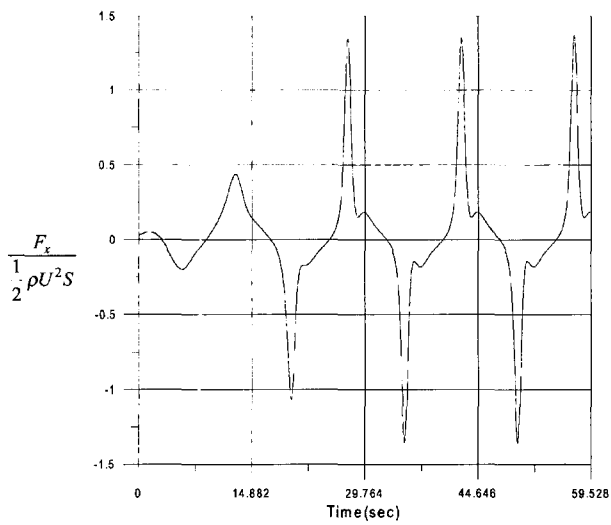


Fig. 6. Impact force on the pillar versus time:  $h=3$  m.

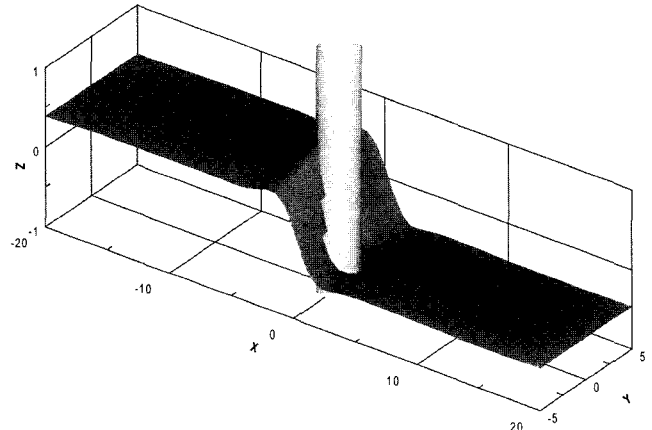


Fig. 8. Wave profile for 1 m depth at  $t=47.1$  sec.

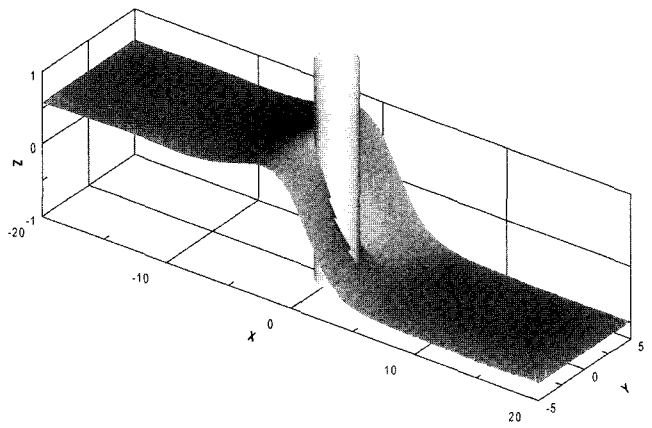


Fig. 9. Wave profile for 2 m depth at  $t=51.6$  sec.

in Table 1. The number of finite elements is taken as 60, 10 and 7 along the length, the width and the depth, respectively. Time integration step is 0.025 sec in average. Total number of elements is 4200. It takes about 9 sec to calculate one time step by PC with 2 GHz Pentium processor.

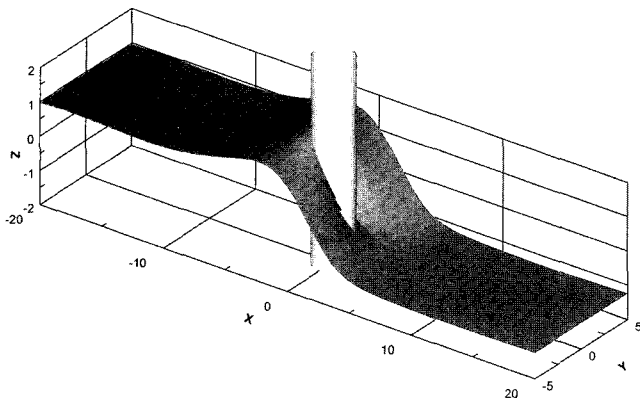


Fig. 10. Wave profile for 3 m depth at  $t=42.4$  sec.

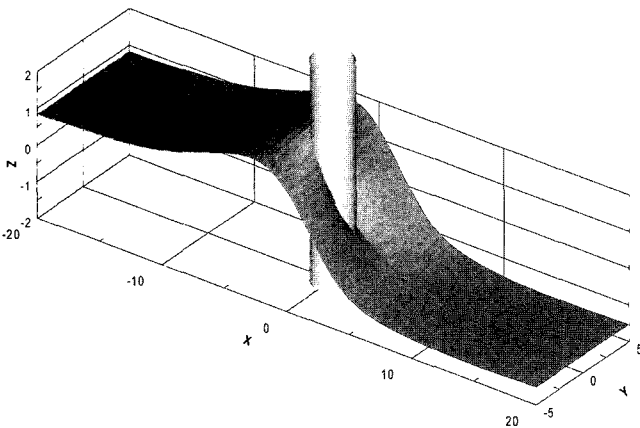


Fig. 11. Wave profile for 4 m depth at  $t=37.1$  sec.

Fig. 4 through Fig. 7 shows the time history of the impact forces. Force acting on the pillar is non-dimensionalized by  $1/2\rho U^2 S$ .  $\rho$  is the density of the fluid. The velocity  $U$  is the critical speed of the bore which equals  $\sqrt{gh}$  in linear shallow-water theory.  $S$  is the projected area namely  $hD$ . In the four different depth cases, it can be observed that the nondimensionalized maximum impact load shows the similar value. The maximum values of non-dimensionalized impact loads lies between 1.0 and 1.4 for the present computed cases. Therefore it seems that the maximum impact load is proportional to the depth squared.

Fig. 8 through Fig. 11 show the wave profiles at the instance of the maximum impact load. Impact loads on the pillar located in the middle of the tank have maximum value when the wave crest hits the pillar. The maximum wave height of bore is observed to be equal to the mean water depth.

So the wave loads increase as the water depth and the height of the bore increases in the cases of the water depth to the length of the tank being relatively low.

As concluding remarks, a series of numerical computations are made for impact load on the pillar in the middle of the shallow filling tank. Very steep bores are observed and they pro-

duce the maximum impact load on the pillar. The maximum wave load is observed when the wave crest hits the pillar.

## ACKNOWLEDGMENTS

This work has been funded partially by both the development of design technology of VLFS funded by MOMAF and the basic research and development program supported by Korea Research Council of Public Science & Technology. This work was also supported by a grant No. (R01-2000-000-00321-0) from Korea Science & Engineering Foundation, the Korea Research Foundation Grant. (KRF-2002-005-D00033), Research Institute of Marine Systems Engineering, College of Engineering, Seoul National University.

## REFERENCES

- [1] Abramson, H.N., Bass, R.L., Faltinsen, O., and Olsen, H.A., 1974, "Liquid slosh in LNG carriers," The 10<sup>th</sup> Symposium on Naval Hydrodynamics, 371-388.
- [2] Adey, B.H. and Caglayan, I., 1982, "The effects of free water on deck on the motions and stability of vessels", Proceedings, 2<sup>nd</sup> international conference on Stability of ships and Ocean vehicles, Tokyo, 413-426.
- [3] Armenio, V. and La Rocca, M., 1996, "On the analysis of sloshing of water in rectangular containers: numerical study and experimental validation", Ocean Engineering, 23(8), 705-739.
- [4] Bai, K.J., Kim, J.W. and Kim, Y.H., 1989, "Numerical Computations For a Nonlinear Free Surface Flow Problem", Proc. 5<sup>th</sup> Int. Conf. on Num. Ship Hydrodynam., Hiroshima, 403-419.
- [5] Bai, K.J., Kim, J.W. and Lee, H.K., 1994, "A Localized Finite Element method for nonlinear free-surface wave problems", Proceedings of the 19<sup>th</sup> Symposium on Naval Hydrodynamics, Hague, Washington, D.C., 113-139.
- [6] Bai, K.J. and Kim, J.W., 1995, "A finite element method for free-surface flow problems", Journal of Theoretical and Applied Mechanics, Vol. 1, No. 1, 1-26.
- [7] Bai, K.J., Kyoung, J.H. and Kim, J.W., 2002, "Numerical Computations for a Nonlinear Free Surface Problem in a Shallow Water", The 21<sup>st</sup> International Conference Offshore Mechanics and Arctic Engineering, Oslo, Norway, 23-28, June, 2002. OMAE2002-28463.
- [8] Chen, W., Haroun, M.A. and Liu, F., 1996, "Large Amplitude liquid sloshing in seismically excited tanks", Earthquake Engineering and Structural Dynamics, 25, 653-669.
- [9] Chester, W., 1968, "Resonant oscillations of water waves. I. Theory", Proceedings, The Royal Society of London, Series A, Vol. 306, 5-22.
- [10] Chester, W. and Bones, J.A., 1968, "Resonant oscillations of water waves. II. Experiments", Proceedings, The Royal Society

of London, Series A, Vol. 306, 23-39.

- [11] Faltinsen, O.M., 1974, "A nonlinear theory of sloshing in rectangular tanks", *Journal of Ship Research*, Vol. 18(4), 224-241.
- [12] Faltinsen, O.M., 1978, "A numerical nonlinear method of sloshing in tanks with two dimensional flow", *Journal of Ship Research*, Vol. 22(3), 193-202.
- [13] Ferrant, P. and Le Touze, D., 2001, "Simulation of sloshing waves in a 3D tank based on a pseudo-spectral method", *Proceedings of 16<sup>th</sup> Int. Workshop on Water Waves and Floating Bodies*, Hiroshima, Japan.
- [14] Huang, Z.J. and Hsiung, C.C., 1996, "Nonlinear shallow-water flow on deck", *Journal of Ship Research*, Vol. 40(4), 303-315.
- [15] Jones, A.F. and Hulme, A., 1987, "The hydrodynamics of water on deck", *Journal of Ship Research*, Vol. 31(2), 125-135.
- [16] Luke, J.C., 1967, "A Variational Principle for a Fluid with a Free Surface", *J. Fluid. Mech.*, 27, 395.
- [17] Miles, J.W., 1977, "On Hamilton's Principle for Surface Waves", *J. Fluid. Mech.*, 83, 395.
- [18] Okamoto, T. and Kawahara, M., 1990, "Two-dimensional sloshing analysis by Lagrangian finite element method", *International Journal for Numerical Methods in Fluids*, Vol. 11, 453-477.
- [19] Saad, Y. and Schultz, M.H., 1986, "GMRES: A Generalized Minimal Residual Algorithm for Solving Nonsymmetric Linear Systems", *SIAM J. Sci. Stat. Comput.*, Vol. 7, 856-869.
- [20] Solaas, F. and Faltinsen, O.M., 1997, "Comnined numerical solution for sloshing in two-dimensional tanks of general shape", *Journal of Ship Research*, Vol. 41, 118-129.
- [21] Ushijim, S., 1998, "Three-dimensional arbitrary Lagrangian - Eulerian numerical prediction method for nonlinear free surface oscillation", *International Journal for Numerical Methods in Fluids*, Vol. 26, 605-623.
- [22] Ven der Bosch, J.J. and Vugts, J.H., 1966, "On roll damping by free-surface tanks", *Transactions, RINA*, Vol. 108, 345-361.
- [23] Verhagen, J.H.G and Wijngaarden, L., 1965, "Nonlinear oscillations of fluid in a container", *Journal of Fluid Mechanics*, Vol. 22, 737-751.
- [24] Wu, G.X., Eatock Taylor, R. and Greaves, 2001, "The effect of viscosity on the transient free-surface waves in a two-dimensional tank", *J. of Eng. Math.*, Vol. 40, 77-90.
- [25] Wu, G.X., Ma, Q.W. and Eatock Taylor, R., 1996, "Analysis of interactions between nonlinear waves and bodies by domain decomposition", *ONR 21<sup>st</sup> Symposium on Naval Hydrodynamics*, Trondheim, Norway, 110-119.
- [26] Zakharov, V.E., 1968, "Stability of Periodic Waves of Finite Amplitude on the Free Surface of a Deep Fluid", *J. Appl. Mech. Tech. Phys.* 9.19.

## APPENDIX

In the present numerical scheme a numerical filtering by using 5-point Chebyshev smoothing algorithm is employed to remove the saw-toothed numerical instability in a time domain analysis. However, there is another difficulty when the computed wave elevation keeps steepening and then the computation can not be continued due to an evident wave breaking. This wave breaking may be real physical phenomena. However, the viscosity which we neglected may play a role of retarding the wave-steepening. Therefore one can compute the steep wave more closely before breaking by introducing a diffusive term in the numerical scheme even though this is not actual simulation of the viscosity.

With this end in mind, we can rewrite the free surface conditions in a form as follows.

$$\zeta_t + C_1(\phi, \zeta)\zeta_x + F(\phi, \zeta) = 0 \quad (\text{A-1})$$

$$\phi_t + C_2(\phi, \zeta)\phi_x + G(\phi, \zeta) = 0 \quad (\text{A-2})$$

If we introduce the diffusive damping term to the RHS (right hand side) as follows.

$$\zeta_t + C_1(\phi, \zeta)\zeta_x + F(\phi, \zeta) = \mu\zeta_{xx} \quad (\text{A-3})$$

$$\phi_t + C_2(\phi, \zeta)\phi_x + G(\phi, \zeta) = \mu\phi_{xx} \quad (\text{A-4})$$

where  $\mu$  is a damping factor. These damping terms may act like a viscous diffusion and prevent the wave profiles from breaking. It is of interest to note that these forms are very similar to the well-known Burgers equation.

---

2004년 8월 10일 원고접수

2004년 10월 25일 수정본 채택